

Cationic Group 14–Platinum(IV) Complexes

Christopher J. Levy, Jagadese J. Vittal, and Richard J. Puddephatt*

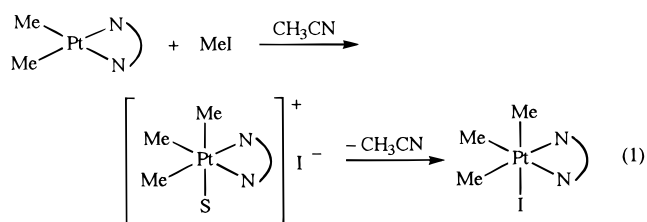
Department of Chemistry, The University of Western Ontario,
London, Ontario, Canada N6A 5B7

Received July 31, 1995[®]

Silver(I) salts abstract halide from $[\text{PtClMe}_2(\text{Me}_2\text{SnCl})(\text{bpy-}^t\text{bu}_2)]$ ($\text{bpy-}^t\text{bu}_2 = 4,4'$ -di-*tert*-butyl-2,2'-bipyridyl), $[\text{PtBrMe}_2(\text{Me}_2\text{SnBr})(\text{bpy-}^t\text{bu}_2)]_2 \cdot \text{Me}_2\text{SnBr}_2$, and $[\text{PtXMe}_2(\text{Me}_3\text{Sn})(\text{bpy-}^t\text{bu}_2)]$ ($\text{X} = \text{Cl, I}$) to form cationic platinum(IV) complexes. $[\text{PtMe}_2(\text{Me}_2\text{SnX})(\text{bpy-}^t\text{bu}_2)]\text{Y}$ ($\text{X} = \text{Cl, Br}$; $\text{Y} = \text{BF}_4, \text{PF}_6$) exists as a 1:1 electrolyte in CH_3CN , probably with solvent coordination to the platinum(IV) cation. The crystal structure of $[\text{PtMe}_2(\text{Me}_2\text{SnCl})(\text{bpy-}^t\text{bu}_2)]\text{BF}_4$ shows a polymeric chain of platinum(IV) cations; the backbone is formed by the coordination of the tin-bound chloro group of one complex to the empty coordination site of an adjacent complex. Bond lengths and angles indicate that the chloro group is largely associated with the tin center, although the tin center displays some stannylene character. VT $^1\text{H-NMR}$ studies show that the cationic species studied undergo rapid exchange processes in solution. Thus, $[\text{PtMe}_2(\text{Me}_2\text{SnCl})(\text{bpy-}^t\text{bu}_2)]^+$ exchanges with $[\text{PtClMe}_2(\text{Me}_2\text{SnCl})(\text{bpy-}^t\text{bu}_2)]$ and $[\text{PtMe}_2(\text{Me}_3\text{Sn})(\text{bpy-}^t\text{bu}_2)]^+$ undergoes rapid exchange processes in the presence of Me_3SnCl .

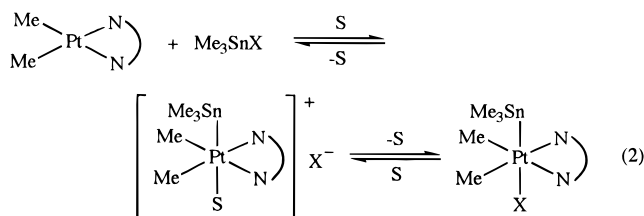
Introduction

An $\text{S}_{\text{N}}2$ mechanism is proposed for the oxidative addition of a variety of electrophilic reagents, including many alkyl halides, to platinum(II) complexes.¹ The initial step in this mechanism gives a cationic platinum(IV) intermediate, which is usually unstable and rapidly captures the halide ion to form a neutral platinum(IV) product. However, in some cases, the cationic platinum(IV) intermediates have been detected by low-temperature NMR spectroscopy, and it was concluded that they exist as solvent-coordinated species (e.g. eq 1; $\text{NN} = 2,2'$ -



bipyridyl (bpy)).^{2,3} Evidence for the existence of a thermodynamically stable cationic intermediate in the reversible oxidative addition of Me_3SnCl to $[\text{PtMe}_2(\text{bpy-}^t\text{bu}_2)]$ has also been obtained (eq 2; $\text{NN} = \text{bpy-}^t\text{bu}_2$, $\text{S} = \text{acetone}$, $\text{X} = \text{Cl, Br, I}$).⁴

Stable cationic organoplatinum(IV) complexes can be generated by halide abstraction from neutral platinum(IV) complexes, often by using silver(I) salts; the low solubility of the resulting silver halide provides the driving force for the reaction. Clark *et al.*⁵ treated a variety of di- and trimethylplatinum(IV) complexes with



silver salts to generate cationic platinum(IV) complexes. The empty coordination site formed on removing the halogen was occupied by a neutral ligand (e.g. PR_3 , RNC) or a coordinating solvent molecule. A number of cationic platinum(IV) complexes, $[\text{PtMe}_2(\text{OR})(\text{NN})(\text{OH}_2)]^+$ ($\text{R} = \text{H, Me, Et, } ^i\text{Pr}$; $\text{NN} = \text{bpy, phenanthroline (phen)}$), have been prepared by the reaction of $[\text{PtMe}_2(\text{NN})]$ with alcohols.⁶ These complexes have a weakly coordinating aqua ligand *trans* to an alkoxy ligand. Recently, Elsevier and co-workers⁷ have reported halide abstraction of $[\text{PtXMe}_2\text{R}(p\text{Tol-BIAN})]$ ($\text{X} = \text{Br, I}$; $\text{R} = \text{Me, Et, PhCH}_2$, acyl, SO_3CF_3 ; $p\text{Tol-BIAN} = (\text{bis}(p\text{-tolylimino})\text{-acenaphthene})$) by silver triflate to form stable platinum(IV) cationic complexes. In solution, the sixth coordination site at platinum was occupied by either a coordinating solvent (CH_3CN) or by the triflate anion. Usually, solvent was not present in the solid state, but if present, it could be removed *in vacuo*. Thus, in the solid state the cation exists either as a true five-coordinate platinum(IV) species or, more likely, an octahedral triflate complex.

The structures of several six-coordinate cationic complexes have been determined,⁸ and it was found that the Pt-L bond lengths were very similar relative to

[®] Abstract published in *Advance ACS Abstracts*, November 1, 1995.

(1) Atwood, J. D. *Inorganic and Organometallic Reaction Mechanisms*; Brooks/Cole: Belmont, 1985; p 172.

(2) Puddephatt, R. J.; Scott, J. D. *Organometallics* **1985**, *4*, 1221.

(3) Crespo, M.; Puddephatt, R. J. *Organometallics* **1987**, *6*, 2548.

(4) Levy, C. J.; Puddephatt, R. J. *J. Chem. Soc., Chem. Commun.*, in press.

(5) (a) Clark, H. C.; Manzer, L. E. *Inorg. Chem.* **1972**, *11*, 2749. (b) Clark, H. C.; Manzer, L. E. *Inorg. Chem.* **1973**, *12*, 362. (c) Appleton, T. G.; Clark, H. C.; Manzer, L. E. *J. Organomet. Chem.* **1974**, *65*, 275.

(6) (a) Monaghan, P. K.; Puddephatt, R. J. *Inorg. Chim. Acta* **1982**, *65*, L59. (b) Monaghan, P. K.; Puddephatt, R. J. *Organometallics* **1984**, *3*, 444.

(7) Asselt, R.; Rijnberg, E.; Elsevier, C. J. *Organometallics* **1994**, *13*, 706.

(8) As examples see: (a) Byers, P. K.; Canty, A. J.; Skelton, B. W.; White, A. H. *J. Chem. Soc., Chem. Commun.* **1987**, 1093. (b) Byers, P. K.; Canty, A. J.; Skelton, B. W.; White, A. H. *Organometallics* **1990**, *9*, 826. (c) Rendina, L. M.; Vittal, J. J.; Puddephatt, R. J. *Organometallics* **1995**, *14*, 1030.

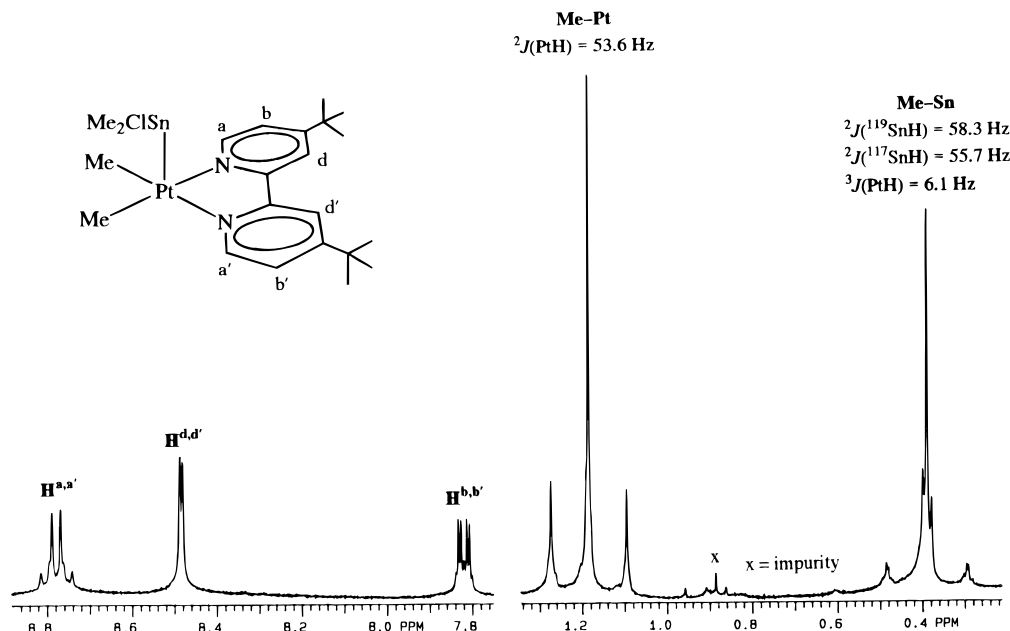
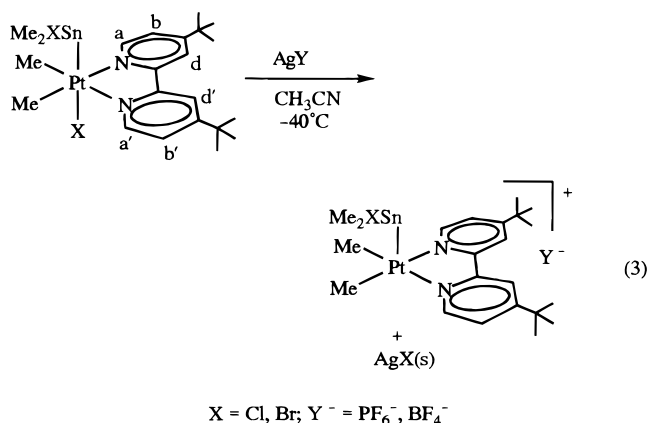


Figure 1. ^1H NMR Spectrum of $[\text{PtMe}_2(\text{Me}_2\text{SnCl})(\text{bpy-}^t\text{bu}_2)]\text{PF}_6$ in CD_3CN at 20°C . The cation is probably solvated.

comparable neutral complexes, indicating that the formal positive charge at platinum does not substantially affect the metal-ligand interactions. In all reported structures there is a ligand of strong *trans* influence occupying the sixth coordination site at platinum. In fact, no crystallographic studies appear to have been reported of five-coordinate organoplatinum(IV) cationic complexes or analogous six-coordinate species where a ligand of very weak *trans* influence occupies the sixth coordination site. Herein we report the first structurally characterized example of the latter and describe halide abstraction reactions of group 14–platinum(IV) complexes to give novel cationic platinum(IV) complexes.

Results

Reactions of $[\text{PtXMe}_2(\text{Me}_2\text{SnX})(\text{bpy-}^t\text{bu}_2)]$ ($\text{X} = \text{Cl}, \text{Br}$) with Silver Salts. The syntheses of the complexes $[\text{PtXMe}_2(\text{Me}_2\text{SnX})(\text{bpy-}^t\text{bu}_2)]$ ($\text{X} = \text{Cl}, \text{Br}$) have been described previously.⁹ Halide abstraction reactions on these complexes using silver(I) reagents, AgPF_6 and AgBF_4 , afford platinum(IV) complexes of composition $[\text{PtMe}_2(\text{Me}_2\text{SnX})(\text{bpy-}^t\text{bu}_2)]\text{PF}_6$ or $[\text{BF}_4]$ (eq 3; $\text{Y}^- = \text{PF}_6^-, \text{BF}_4^-$). A solvent molecule is likely to be coordinated weakly *trans* to tin; the NMR labeling scheme is shown). The reactions are sensitive to temperature and the nature of the solvent. Upon addition of silver(I) salt to cold solutions of $[\text{PtXMe}_2(\text{Me}_2\text{SnX})(\text{bpy-}^t\text{bu}_2)]$ ($\text{X} = \text{Cl}, \text{Br}$), there is an immediate color change from yellow to colorless and the reaction is accompanied by the formation of $\text{AgX}(\text{s})$. The solution must be filtered to remove the silver halide and the solvent removed as quickly as possible to isolate the product. Once the pure product is isolated, it is robust in solution; little decomposition was evident by ^1H NMR for a solution of $[\text{PtMe}_2(\text{Me}_2\text{SnCl})(\text{bpy-}^t\text{bu}_2)]\text{PF}_6$ in CD_3CN at 0°C after 20 h. We have carried out the halide abstraction reactions in CH_2Cl_2 , acetone, THF, and CH_3CN and have found that CH_3CN gives the best results



and purest products. The molar conductivity of pure $[\text{PtMe}_2(\text{Me}_2\text{SnCl})(\text{bpy-}^t\text{bu}_2)]\text{PF}_6$ in CH_3CN ($\Lambda = 154 \text{ S cm}^2 \text{ mol}^{-1}$) is within the $120\text{--}160 \text{ S cm}^2 \text{ mol}^{-1}$ range expected for a 1:1 electrolyte in CH_3CN .¹⁰ Of course, it is likely that the sixth coordination site is occupied by a very weakly coordinated solvent molecule in solution, but it is noteworthy that the isolated products did not contain coordinated solvent. The question then arises as to whether the anions (which have very poor coordinating properties toward soft metal ions) may occupy the sixth site in the solid-state structures or if these are really five-coordinate cations, favored by the very strong *trans* influence of the heavy group 14 donor atom.

The ^1H NMR spectrum of $[\text{PtMe}_2(\text{Me}_2\text{SnCl})(\text{bpy-}^t\text{bu}_2)]\text{PF}_6$ in CD_3CN is shown in Figure 1 (the *tert*-butyl signal is omitted for the sake of clarity). The Me–SnPt signal clearly shows both tin and platinum satellites. The chemical shift of the signal is 0.38 ppm and is to high frequency of the corresponding signal in $[\text{PtClMe}_2(\text{Me}_2\text{SnCl})(\text{bpy-}^t\text{bu}_2)]$ in CD_3CN (0.27 ppm). The value of $^2J(^{119}\text{SnH})$ for the methyltin resonance increased from 53.5 Hz for $[\text{PtClMe}_2(\text{Me}_2\text{SnCl})(\text{bpy-}^t\text{bu}_2)]$ to 58.3 Hz for the cationic complex. The ^1H NMR spectra of the cationic Pt(IV) complex in solution in CD_3CN at temperatures from -40 to 20°C were not affected by the

(9) Levy, C. J.; Vittal, J. J.; Puddephatt, R. J. *Organometallics*, submitted for publication.

(10) Geary, W. J. *Coord. Chem. Rev.* **1971**, 7, 81.

Table 1. Crystallographic Details for [PtMe₂(Me₂SnCl)(bpy-*t*bu₂)]BF₄

formula	C ₂₂ H ₃₆ BClF ₄ N ₂ PtSn
fw	764.59
T, K	298
λ, Å	0.710 73
space group	P2 ₁
a, Å	11.032(2)
b, Å	11.733(1)
c, Å	11.681(2)
β, deg	113.57(1)
V, Å ³	1385.8(5)
Z	2
ρ _{calcd} , g cm ⁻³	1.83
ρ _{obsd} , g cm ⁻³	1.85(5)
μ, mm ⁻¹	6.1
F(000)	736
NO ^a	2804 [F _o ≥ 4σ(F _o)]
R ^b	0.0459
R _w ^c	0.1074
S ^d	1.049

^a NO = number of observed reflections. ^b R = Σ(|F_o| - |F_c|)/Σ|F_o|. ^c R_w = [Σw(F_o² - F_c²)²/ΣwF_o⁴]^{1/2}. ^d S = Goodness of fit; S = [Σw(|F_o| - |F_c|)²/(M - N)]^{1/2}, where M is the number of reflections and N is the number of parameters refined.

presence of Me₂SnCl₂, indicating that there are no rapid exchange processes (either reversible reductive elimination of the tin fragment or abstraction of chloride from free Me₂SnCl₂). However, in another ¹H NMR study, a 1:1 mixture of [PtClMe₂(Me₂SnCl)(bpy-*t*bu₂)] and [PtMe₂(Me₂SnCl)(bpy-*t*bu₂)]PF₆ was shown to give only one broad Me–Sn signal, while the value of ²J(PtH) for the Me–Pt signal was 55.0 Hz, close to the value of 55.2 Hz expected for a rapidly exchanging mixture of [PtClMe₂(Me₂SnCl)(bpy-*t*bu₂)] (56.7 Hz) and [PtMe₂(Me₂SnCl)(bpy-*t*bu₂)]PF₆ (53.6 Hz). This observation indicates that the Pt–Cl bond trans to tin is labile and the chloride is easily and reversibly abstracted by the cationic platinum center. Evidently, if the sixth coordination site of the cationic platinum(IV) center in solution is occupied by solvent, then very rapid dissociation must be possible to permit the halide abstraction to occur.

X-ray Crystal Structure of [PtMe₂(Me₂SnCl)(bpy-*t*bu₂)]BF₄. X-ray-quality crystals of the BF₄⁻ salt were successfully grown by slow diffusion of pentane into a CH₂Cl₂ solution of the salt over a 3-week period (–30 °C). The X-ray structure of the crystal was determined, and the experimental details are presented in Table 1. Atomic coordinates are presented in Table 2, and bond lengths and angles are contained in Table 3. Figure 2 shows the structural diagram of three adjacent platinum(IV) units along with the atom-labeling scheme. Approximately octahedral coordination geometries about the platinum centers result from the coordination of the chloride from the Me₂SnCl ligand to the platinum center of an adjacent cation. The bpy-*t*bu₂ ligand displays no exceptional features, and the *tert*-butyl groups have a 2-fold disorder as described previously for [PtIME₂(Me₃Sn)(bpy-*t*bu₂)].⁹ The BF₄⁻ counterions occupy lattice positions that do not allow interaction with the platinum center. There is a 2-fold disorder, in each BF₄⁻ ion, and the shortest F...Sn contacts are 3.423 Å. The most interesting feature of the structure of [PtMe₂(Me₂SnCl)(bpy-*t*bu₂)]BF₄ is the presence of a polymeric chain structure with a Pt–Sn–Cl–Pt backbone. The polymer has an alternating configuration, with bpy-*t*bu₂ ligands of every second platinum(IV) unit

Table 2. Atomic coordinates (×10⁴) and Equivalent Isotropic Displacement Parameters (Å² × 10³)

atom	x	y	z	U _{eq} ^a
Pt(1)	–859.7(6)	2500	4578.0(5)	41.2(2)
Sn(1)	–2128(1)	4234(1)	4801(1)	49(1)
Cl(1)	–251(6)	5496(4)	5874(5)	65(1)
C(1)	–626(18)	3306(18)	3082(14)	55(5)
C(2)	–2670(18)	1893(18)	3315(17)	60(5)
C(3)	–2846(29)	3983(26)	6194(24)	102(9)
C(4)	–3267(24)	5171(19)	3192(20)	83(7)
N(1)	1046(11)	2906(12)	5920(11)	40(3)
N(2)	–850(12)	1705(12)	6240(11)	37(3)
C(5)	1987(16)	3402(17)	5677(15)	46(4)
C(6)	3223(18)	3653(18)	6638(16)	55(5)
C(7)	3489(16)	3375(17)	7832(15)	48(4)
C(8)	2517(14)	2821(15)	8089(14)	47(4)
C(9)	1296(12)	2572(21)	7113(11)	35(3)
C(10)	258(14)	1937(15)	7289(13)	39(3)
C(11)	364(17)	1487(17)	8441(15)	52(4)
C(12)	–660(16)	839(17)	8533(14)	49(4)
C(13)	–1773(19)	643(19)	7456(17)	61(5)
C(14)	–1807(17)	1086(17)	6321(16)	52(4)
C(15)	4881(10)	3583(10)	8918(11)	59(5)
C(16)	5853(20)	2791(17)	8655(24)	106(12)
C(17)	5287(26)	4832(11)	8876(27)	94(11)
C(18)	4910(29)	3316(25)	10219(19)	94(11)
C(16A)	5913(28)	3465(31)	8346(33)	89(24)
C(17A)	4880(48)	4816(16)	9367(44)	77(22)
C(18A)	5229(42)	2762(32)	10032(29)	62(16)
C(19)	–482(11)	362(11)	9815(12)	63(5)
C(20)	786(15)	865(24)	10820(26)	67(10)
C(21)	–1686(17)	733(30)	10076(34)	108(18)
C(22)	–389(32)	–948(12)	9843(36)	103(17)
C(20A)	510(24)	–622(19)	10039(37)	79(13)
C(21A)	27(32)	1186(29)	10933(29)	105(17)
C(22A)	–1833(19)	–122(26)	9670(39)	102(17)
B(1)	–3861(21)	–2446(24)	6586(21)	153(15)
F(1)	–2603(25)	–2129(35)	6782(31)	175(8)
F(2)	–4605(34)	–1510(29)	6600(34)	175(8)
F(3)	–4449(33)	–3037(30)	5485(25)	175(8)
F(4)	–3834(32)	–3175(31)	7528(28)	175(8)
F(1A)	–2933(47)	–3011(50)	6265(50)	217(17)
F(2A)	–4009(54)	–1352(34)	6074(59)	217(17)
F(3A)	–5041(38)	–3023(43)	6055(54)	217(17)
F(4A)	–3435(49)	–2372(65)	7851(28)	217(17)

^a U_{eq} is defined as one-third of the trace of the orthogonalized U_{ij} tensor. The multiplicity factors for C(16), C(17), C(18) and C(16A), C(17A), C(18A) are 0.7 and 0.3, respectively, for C(20), C(21), C(22) and C(20A), C(21A), C(22A) are 0.5 and 0.5, respectively, and for F(1) to F(4) and F(1A) to F(4A) are 0.6 and 0.4, respectively.

being in an eclipsed conformation. This effect is likely due to the bulky nature of the bpy-*t*bu₂ ligands, which does not favor their alignment in adjacent complexes.

Generation and Study of [PtMe₂(Me₃E)(bpy-*t*bu₂)]⁺ (X = Cl, Br, I; E = Si, Sn). The complexes [PtXMe₂(Me₃Sn)(bpy-*t*bu₂)] (X = Cl, I) reacted with silver salts in acetonitrile solution in a manner similar to that for [PtXMe₂(Me₂SnX)(bpy-*t*bu₂)] (X = Cl, Br), but the (probably solvated) cation [PtMe₂(Me₃Sn)(bpy-*t*bu₂)]⁺ decomposed slowly in solution, so that analytically pure products could not be obtained. The products were therefore characterized in solution by ¹H NMR spectroscopy. The reactions of [PtMe₂(bpy-*t*bu₂)] with Me₃SnBF₄ (generated *in situ* by the addition of AgBF₄ to Me₃SnCl) and of [PtIME₂(Me₃Sn)(bpy-*t*bu₂)] with AgBF₄ gave products whose ¹H NMR spectra were identical, indicating that in both cases the (probably solvated) cation [PtMe₂(Me₃Sn)(bpy-*t*bu₂)]⁺ is formed. The spectral parameters of the cation are very similar to those of the parent complexes, [PtXMe₂(Me₃Sn)(bpy-*t*bu₂)] (X = Cl, Br, I), with minor changes in chemical shifts and

Table 3. Bond Lengths (Å) and Angles (deg)^a

Bond Lengths							
Pt(1)–Sn(1)	2.541(2)	Pt(1)–Cl(1)#1	2.798(5)	C(7)–C(15)	1.57(2)	C(8)–C(9)	1.40(2)
Pt(1)–N(1)	2.114(12)	Pt(1)–N(2)	2.150(12)	C(9)–C(10)	1.45(2)	C(10)–C(11)	1.41(2)
Pt(1)–C(1)	2.092(16)	Pt(1)–C(2)	2.077(17)	C(11)–C(12)	1.40(2)	C(12)–C(13)	1.38(2)
Sn(1)–C(3)	2.097(20)	Sn(1)–C(4)	2.105(21)	C(12)–C(19)	1.54(2)	C(13)–C(14)	1.41(2)
Sn(1)–Cl(1)	2.444(5)	N(1)–C(5)	1.32(2)	B(1)–F(4A)	1.36(2)	B(1)–F(1)	1.37(2)
N(1)–C(9)	1.37(2)	N(2)–C(10)	1.37(2)	B(1)–F(3A)	1.37(2)	B(1)–F(3)	1.37(2)
N(2)–C(14)	1.32(2)	C(5)–C(6)	1.41(2)	B(1)–F(2)	1.37(2)	B(1)–F(4)	1.38(2)
C(6)–C(7)	1.34(2)	C(7)–C(8)	1.39(2)	B(1)–F(1A)	1.39(2)	B(1)–F(2A)	1.40(2)
Bond Angles							
N(1)–Pt(1)–Sn(1)	99.7(4)	N(2)–Pt(1)–Sn(1)	93.4(3)	C(18A)–C(15)–C(16A)	109.5(1)	C(17A)–C(15)–C(16A)	109.5(1)
C(2)–Pt(1)–Sn(1)	86.3(6)	C(1)–Pt(1)–Sn(1)	88.9(5)	C(17)–C(15)–C(7)	109.0(14)	C(16)–C(15)–C(7)	106.2(12)
N(1)–Pt(1)–N(2)	77.5(5)	N(1)–Pt(1)–N(1)	173.0(7)	C(18)–C(15)–C(7)	113.2(14)	C(16A)–C(15)–C(7)	107(2)
C(1)–Pt(1)–N(1)	95.7(6)	C(2)–Pt(1)–N(2)	98.5(7)	C(17A)–C(15)–C(7)	107(2)	C(18A)–C(15)–C(7)	115(2)
C(1)–Pt(1)–N(2)	173.1(6)	C(2)–Pt(1)–C(1)	88.1(8)	C(22)–C(19)–C(21)	109.5(1)	C(22)–C(19)–C(20)	109.5(1)
Sn(1)–Pt(1)–Cl(1)#1	173.2(1)	N(1)–Pt(1)–Cl(1)#1	87.1(4)	C(21)–C(19)–C(20)	109.5(1)	C(20A)–C(19)–C(21A)	109.5(1)
N(2)–Pt(1)–Cl(1)#1	87.8(4)	C(2)–Pt(1)–Cl(1)#1	87.0(6)	C(20A)–C(19)–C(22A)	109.5(1)	C(21A)–C(19)–C(22A)	109.5(1)
C(1)–Pt(1)–Cl(1)#1	90.7(5)	Cl(1)–Sn(1)–Pt(1)	98.6(1)	C(12)–C(19)–C(22)	111(2)	C(12)–C(19)–C(21)	108(2)
C(3)–Sn(1)–Pt(1)	111.2(8)	C(4)–Sn(1)–Pt(1)	118.9(7)	C(12)–C(19)–C(20)	109(2)	C(12)–C(19)–C(20A)	104(2)
C(3)–Sn(1)–Cl(1)	101.1(8)	C(4)–Sn(1)–Cl(1)	102.8(7)	C(12)–C(19)–C(21A)	117(2)	C(12)–C(19)–C(22A)	107(2)
C(3)–Sn(1)–C(4)	119.4(11)	Sn(1)–Cl(1)–Pt(1)#2	139.2(2)	F(4A)–B(1)–F(1)	85(3)	F(4A)–B(1)–F(3A)	112(2)
C(5)–N(1)–C(9)	119.5(13)	C(5)–N(1)–Pt(1)	125.2(10)	F(1)–B(1)–F(3A)	158(2)	F(4A)–B(1)–F(3)	151(3)
C(9)–N(1)–Pt(1)	115.3(9)	C(14)–N(2)–C(10)	120.0(13)	F(1)–B(1)–F(3)	111(2)	F(3A)–B(1)–F(3)	47(2)
C(14)–N(2)–Pt(1)	126.2(10)	C(10)–N(2)–Pt(1)	113.7(10)	F(4A)–B(1)–F(2)	83(3)	F(1)–B(1)–F(2)	111(2)
N(1)–C(5)–C(6)	121.1(16)	C(7)–C(6)–C(5)	121.1(18)	F(3A)–B(1)–F(2)	86(2)	F(3)–B(1)–F(2)	111(2)
C(6)–C(7)–C(8)	118.1(16)	C(6)–C(7)–C(15)	122.5(15)	F(4A)–B(1)–F(4)	45(3)	F(1)–B(1)–F(4)	110(2)
C(8)–C(7)–C(15)	119.3(13)	C(7)–C(8)–C(9)	119.8(14)	F(3A)–B(1)–F(4)	77(3)	F(3)–B(1)–F(4)	106(2)
N(1)–C(9)–C(8)	120.3(14)	N(1)–C(9)–C(10)	116.4(12)	F(2)–B(1)–F(4)	108(2)	F(4A)–B(1)–F(1A)	110(2)
C(8)–C(9)–C(10)	123.2(13)	N(2)–C(10)–C(11)	119.0(15)	F(1)–B(1)–F(1A)	51(2)	F(3A)–B(1)–F(1A)	108(2)
N(2)–C(10)–C(9)	116.7(12)	C(11)–C(10)–C(9)	124.2(13)	F(3)–B(1)–F(1A)	68(2)	F(2)–B(1)–F(1A)	153(3)
C(12)–C(11)–C(10)	121.0(15)	C(13)–C(12)–C(11)	118.1(16)	F(4)–B(1)–F(1A)	98(3)	F(4A)–B(1)–F(2A)	110(2)
C(13)–C(12)–C(19)	123.2(16)	C(11)–C(12)–C(19)	118.6(13)	F(1)–B(1)–F(2A)	76(3)	F(3A)–B(1)–F(2A)	109(2)
C(12)–C(13)–C(14)	118.3(18)	N(2)–C(14)–C(13)	123.5(16)	F(3)–B(1)–F(2A)	98(3)	F(2)–B(1)–F(2A)	46(3)
C(17)–C(15)–C(16)	109.5(1)	C(17)–C(15)–C(18)	109.5(1)	F(4)–B(1)–F(2A)	150(3)	F(1A)–B(1)–F(2A)	107(2)
C(16)–C(15)–C(18)	109.5(1)	C(18A)–C(15)–C(17A)	109.5(1)				

^a Symmetry transformations used to generate equivalent atoms: (#1) $-x, y - 1/2, -z + 1$; (#2) $-x, y + 1/2, -z + 1$. Close Nonbonded Contacts (Å): F(3A)···H(2A), 2.232 ($-x - 1, y - 0.5, 1 - z$); F(2)···H(4B), 2.406 ($-x - 1, y - 0.5, 1 - z$); F(2)···Sn(1), 3.423 ($-x - 1, y - 0.5, 1 - z$); H(5)···F(1), 2.530 ($-x, y + 0.5, 1 - z$).

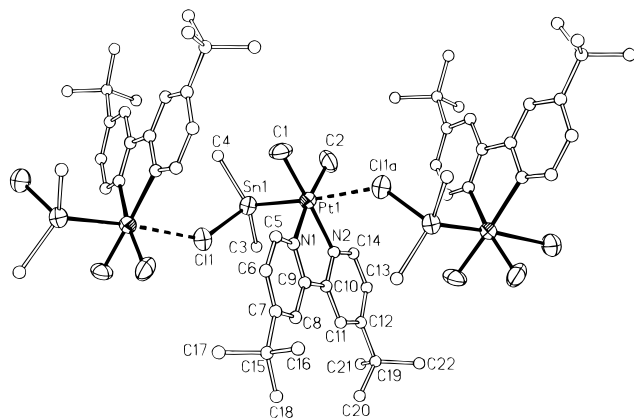


Figure 2. View of $[\text{PtMe}_2(\text{Me}_2\text{SnCl})(\text{bpy}-4\text{bu}_2)]\text{BF}_4$ showing interactions of cationic units. Thermal ellipsoids are represented at the 50% probability level.

coupling constants. One notable difference is the sharpness of the signals of $[\text{PtMe}_2(\text{Me}_3\text{Sn})(\text{bpy}-4\text{bu}_2)]^+$ at room temperature compared to those of the parent complexes.¹⁰

Analogous cationic silylplatinum(IV) complexes appear to be much less stable. Thus, reaction of $[\text{PtMe}_2(\text{Me}_3\text{Si})(\text{bpy}-4\text{bu}_2)]$ with silver salts at low temperature in CH_3CN or THF solution resulted in an initial color change from bright yellow to colorless, indicative of formation of the cationic complex, but the solution quickly darkened and the ^1H NMR spectra contained several Me–Si signals (0.0–0.2 ppm) and several sets of signals due to the $\text{bpy}-4\text{bu}_2$ ligand, but no major Me–Pt signal. The spectra indicate complete decomposition of the cationic silylplatinum(IV) complex to give a

number of products. The signal at 0.0 ppm is indicative of formation of Me_4Si and implies at least partial decomposition of $[\text{PtMe}_2(\text{Me}_3\text{Si})(\text{bpy}-4\text{bu}_2)]^+$ by reductive elimination of Me_4Si .

Discussion

Several cationic stannylplatinum(IV) complexes have been prepared by halide abstraction using silver(I) salts. In several cases pure samples of the salts could be isolated and the products were reasonably robust even in solution. However, in other cases, the cationic platinum(IV) complexes decomposed prior to isolation, even when reactions were carried out at low temperature in coordinating solvents. The tendency for decomposition of the cationic platinum(IV) species compared to the neutral starting materials is a result of the effects of positive charge and coordinative unsaturation. It has been demonstrated that the rate of reductive elimination from organoplatinum(IV) complexes increases when a charged¹¹ or coordinatively unsaturated species is generated.^{5,12} This work indicates that the cationic stannylplatinum(IV) complexes generated by the halide abstraction reactions are similarly susceptible to decomposition by irreversible reductive-elimination reactions.

The complexes $[\text{PtXMe}_2(\text{Me}_2\text{SnX})(\text{bpy}-4\text{bu}_2)]$ ($X = \text{Cl}, \text{I}$) contain two halo ligands, one on the platinum and one on the tin, which in principle can be removed by reaction with a silver salt. The Pt–X bond is more

(11) Ettore, R. *Inorg. Nucl. Chem. Lett.* **1969**, 5, 45.

(12) Brown, M. P.; Puddephatt, R. J.; Upton, C. E. E.; Lavington, S. W. *J. Chem. Soc., Dalton Trans.* **1974**, 1613.

Table 4. Platinum–Chlorine Bond Lengths

complex	Pt–Cl bond length (Å)	ref
[PtMe ₂ (Me ₂ SnCl)(bpy- ⁴ bu ₂)]BF ₄	2.798(5)	
[PtClMe ₂ (RCH=NCH ₂ CH ₂ NMe ₂)]	2.456(3)	16
[PtCl(Ph ₂ SnCl)(C ₂ H ₄)(dmphen)]	2.478(3)	17
[PtCl(SnCl ₃)(<i>p</i> -Cl-C ₆ H ₄ NH ₂)(PEt ₃)]	2.331(3)	15a
av for bridging chloro ligand	2.410(6)	18
[C ₉ H ₈ N] ₂ [Pt(μ -Cl)Cl ₃ (NO)] ₂	2.742 (<i>r</i> ² = 0.101)	19
[Pt(μ -Cl)Et ₃] ₄	2.714	15c
<i>sym-trans</i> -[Pt(SnCl ₃)(μ -Cl)(PEt ₃) ₂]	2.35(1)	15b

reactive to halide abstraction than the Sn–X bond, probably due to the very strong *trans* effect of a group 14 ligand. Abstraction of the tin-bound chloride can potentially lead to the formation of a stannylen complex. However, the ¹H NMR spectrum of the product resulting from the addition of 2 equiv of silver(I) to a solution of [PtClMe₂(Me₂SnCl)(bpy-⁴bu₂)] was identical with that obtained from the addition of 1 equiv, indicating that the Sn–Cl bond cannot be cleaved by reaction with silver(I). Similarly, attempts to abstract all bromide ligands from [PtBrMe₂(Me₂SnBr)(bpy-⁴bu₂)]₂·Me₂SnBr₂ were unsuccessful. Thus, it appears that only one halide ion can be removed from [PtXMe₂(Me₂SnX)(bpy-⁴bu₂)] (X = Cl, Br) by use of the silver reagents employed in this work.

The successful synthesis of cationic platinum(IV) species is largely dependent on the solvent employed. The favorable results in CH₃CN can be attributed to the stabilizing effect of weak coordination of CH₃CN to the cationic platinum(IV) complexes,¹³ with complete ionization of the counterions BF₄⁻ and PF₆⁻.¹⁴ Molar conductivity results confirm that the salt forms a 1:1 electrolyte in acetonitrile. In contrast, elemental analyses and X-ray crystallography clearly show that CH₃CN is not present in the solid state of [PtMe₂(Me₂SnX)(bpy-⁴bu₂)]Y (X = Cl, Br; Y = BF₄⁻, PF₆⁻), and ¹H NMR shows that CH₃CN is not incorporated into [PtMe₂(Me₃Sn)(bpy-⁴bu₂)]Y (Y = BF₄⁻, PF₆⁻). Elsevier and co-workers⁷ have synthesized platinum(IV) cationic species in CH₃CN and found solvent incorporation. However, the solvent could be removed *in vacuo*, indicating that it was loosely held within the crystal lattice. Their solution studies concluded that CH₃CN did not have a strong tendency to coordinate to the platinum(IV) cationic species when compared to the triflate anion. For our complexes in the solid state, it appears that occupation of the sixth coordination site at platinum by a weakly bound halo ligand of an adjacent platinum(IV) unit is favored over CH₃CN coordination or coordination of the anions.

Crystallographic studies show that there are no significant differences in the Me–Pt and Me–Sn bond lengths of [PtMe₂(Me₂SnCl)(bpy-⁴bu₂)]BF₄ compared to those of [PtIme₂(Me₃Sn)(bpy-⁴bu₂)].⁹ This indicates that there is little difference in the nature of the platinum(IV) centers despite the formal cationic nature of the former. This is consistent with the observation that the ¹H NMR spectrum changes only marginally upon the reaction of [PtClMe₂(Me₂SnCl)(bpy-⁴bu₂)] with silver(I). The bent Sn–Cl–Pt angle (139.2°) between two [PtMe₂(Me₂SnCl)(bpy-⁴bu₂)]⁺ units is indicative of a bridging chloro ligand. Table 4 compares the observed

Pt–Cl bond length with those in some known complexes. The Pt–Cl distance (2.798(5) Å) is long in comparison to the known range for single Pt–Cl bonds *trans* to a ligand of strong *trans* influence;¹⁵ it is over 0.3 Å longer than the Pt–Cl bonds in [PtClMe₂(RCH=NCH₂CH₂NMe₂)] (R = *o*-ClC₆H₃ with *o*-carbon coordination to platinum)¹⁶ and [PtCl(Ph₂SnCl)(C₂H₄)(dmphen)],¹⁷ where the chloro ligand is *trans* to a methyl and a Ph₂SnCl ligand, respectively. This difference is far greater than could be accounted for by the larger *trans* influence of the Me₂SnCl compared to the Ph₂SnCl or Me ligands. A survey of published structures reveals that bridging chloro ligands generally have longer Pt–Cl bonds than terminal chloro ligands.¹⁸ Table 4 shows that the Pt–Cl bond length we observe is longer than the longest bridging Pt–Cl bonds reported.¹⁹ Our conclusion is that the bridging chloro ligand in [PtMe₂(Me₂SnCl)(bpy-⁴bu₂)]BF₄ is largely associated with the tin center and that there is a very weak interaction with the platinum center of the adjacent complex. A weak platinum–halide interaction has been established for some complexes which contain both platinum(II) and platinum(IV) units in the solid state. [Pt(NH₂Et)₄Cl₂][Pt(NH₂Et)₄Cl₄] has a weak bridging interaction (the Pt···Cl distance is 3.13 Å) between the chloro ligand of a platinum(IV) unit and an adjacent Pt(II) unit.²⁰ [Pt(en)Br₃] has a similar solid-state structure, with a Pt^{II}···Br distance of 3.125 Å.²¹ These structures have a halo ligand weakly coordinated to the unoccupied coordination sites of a platinum(II) center. This is a distinctly different interaction than is present in [PtMe₂(Me₂SnCl)(bpy-⁴bu₂)]BF₄, where the chloro ligand is weakly coordinated to the sixth coordination site of a platinum(IV) complex.

The geometry at the tin center is distorted tetrahedral. The C–Sn–Pt angles are both opened up from those in an ideal tetrahedron, while the Cl–Sn–Pt angle is significantly smaller than that in an ideal geometry. At the tin center, we see that the C–Sn–Cl angles are smaller than those in an ideal tetrahedron, while the C–Sn–C angle is larger. The latter is close to 120°. MacKay and Nicholson²² have noted that the geometry at the group 14 element in most R₃E–TM complexes (E = Si, Ge, Sn, Pb, TM = transition metal) is distorted from tetrahedral. Generally, the TM–E–R angle is in the range 113–119° with corresponding decreases in R–E–R of *ca.* 5° from tetrahedral. The smallest R–E–R angles occur with more electronegative groups. The C–Sn–Pt and C–Sn–Cl angles of the Me₂SnCl

(15) (a) Albinati, A.; Moriyama, H.; Rügger, H.; Pregosin, P. S. *Inorg. Chem.* **1985**, *24*, 4430. (b) Albinati, A.; Naegeli, R.; Starzewski, O.; Pregosin, P. S.; Rügger, H. *Inorg. Chim. Acta* **1983**, *76*, L232. (c) Hargraves, M. R.; Truter, M. J. *J. Chem. Soc. A* **1971**, 90.

(16) Anderson, C. M.; Crespo, M.; Jennings, M. C.; Lough, A. J.; Ferguson, G.; Puddephatt, R. J. *Organometallics* **1991**, *10*, 2672.

(17) Albano, V. G.; Castellari, C.; Felice, V.; Panunzi, A.; Ruffo, F. *J. Organomet. Chem.* **1992**, *425*, 177.

(18) Determined by a search of the Cambridge Structural Database (to Oct 1993). The GSTAT program was used to find Pt–Cl (bridging) bond lengths and determine the mean value: mean (from 208 bonds in 87 structures), 2.410 Å; standard deviation of sample, 0.088 Å; standard deviation of mean, 0.006 Å; minimum, 2.284 Å; maximum, 2.742 Å.

(19) Khodashova, T. S.; Sergienko, V. S.; Stetsenko, A. N.; Porai-Koshits, M. A.; Butman, L. A. *Zh. Strukt. Khim.* **1974**, *15*, 471.

(20) Craven, B. M.; Hall, D. *Acta Crystallogr.* **1961**, *14*, 475.

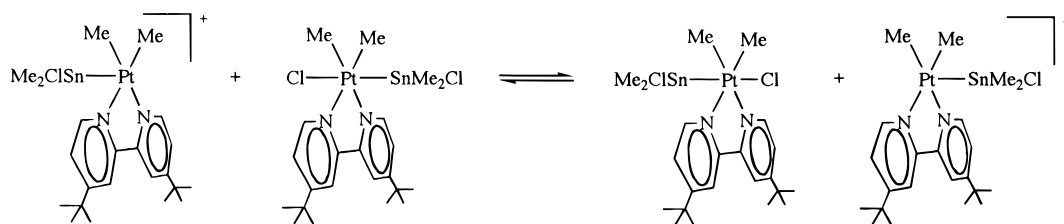
(21) Ryan, T. D.; Rundle, R. E. *J. Am. Chem. Soc.* **1961**, *83*, 2814.

(22) McKay, K. M.; Nicholson, B. K. *Comprehensive Organometallic Chemistry*; Wilkinson, G., Stone, F. G. A., Abel, E. W., Eds.; Pergamon: Oxford, U.K., 1982; Vol. 6, p 1106.

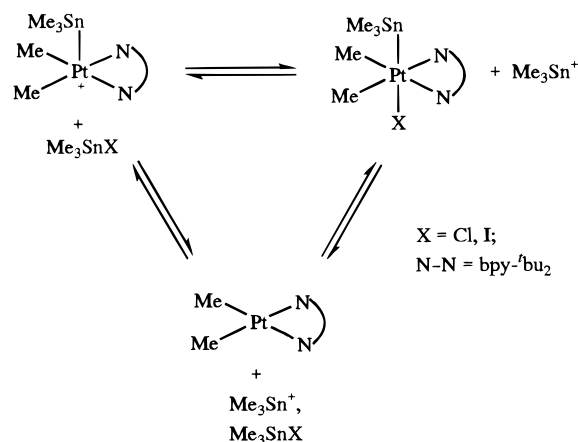
(13) Hartley, F. R. *The Chemistry of Platinum and Palladium*; Applied Science Publishers: London, 1973; pp 307–308.

(14) Beck, W.; Sünkel, K. *Chem. Rev.* **1988**, *88*, 1405.

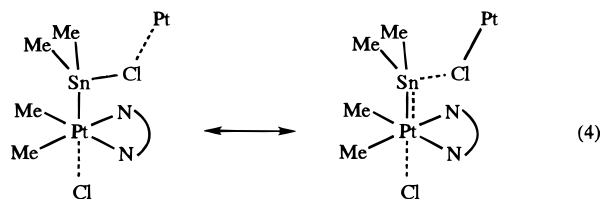
Scheme 1



Scheme 2



group in $[\text{PtMe}_2(\text{Me}_2\text{SnCl})(\text{bpy-}^4\text{bu}_2)]\text{BF}_4$ are consistent with these trends, but the small Cl-Sn-Pt and large C-Sn-C angles seem anomalous. Onaka²³ has reported the structure of $[\text{Mn}(\text{Me}_2\text{SnBr})(\text{CO})_3(\text{PPh}_3)_2]$, which contains a Me_2SnBr ligand; the Br-Sn-Mn and C-Sn-C angles are $112.3(2)$ and $102.0(13)^\circ$, respectively. Recently, the structure of $[\text{PtCl}(\text{SnPh}_2\text{Cl})(\text{C}_2\text{H}_4)(\text{dmphen})]$ ¹⁷ has been reported and shows Cl-Sn-Pt and C-Sn-C angles of $108.0(1)$ and $110.2(4)^\circ$, respectively. Neither of these structures show parallels to the anomalously small Cl-Sn-Pt and large C-Sn-C bond angles observed in $[\text{PtMe}_2(\text{Me}_2\text{SnCl})(\text{bpy-}^4\text{bu}_2)]\text{BF}_4$. The distortions seen at the tin center in the cation are consistent with some stannylene character in the Pt-Sn interaction. Stannylene character should be accompanied by a shortened Pt-Sn bond, but there are no structures published which allow direct comparisons. Stannylene character in the Me_2SnCl ligand of $[\text{PtMe}_2(\text{Me}_2\text{SnCl})(\text{bpy-}^4\text{bu}_2)]\text{BF}_4$ should be reflected by a longer than expected Sn-Cl bond length. The observed Sn-Cl bond length ($2.444(5)$ Å) is somewhat longer than that observed in $[\text{PtCl}(\text{SnPh}_2\text{Cl})(\text{C}_2\text{H}_4)(\text{dmphen})]$ ($2.393(3)$ Å).¹⁷ The difference in Sn-Cl bond lengths between these complexes ($0.051(6)$ Å) is significantly larger than that observed between Me_2SnCl_2 and Ph_2SnCl_2 (<0.01 Å).^{24,25} Thus, the difference in Sn-Cl bond lengths does not appear to be due to a change in organic groups on tin but, of course, could be due to the weak bridging to a neighboring platinum atom. Thus, the structural evidence, though not compelling, is consistent with *some* stannylene character in the Me_2SnCl ligand (eq 4). The chemistry, especially the inability to abstract the halide from tin, suggests that the stannylene character is relatively minor.



¹H NMR studies provide information regarding the bonding in the cationic complexes in solution. Overall, the spectrum of the platinum(IV) cation $[\text{PtMe}_2(\text{Me}_2\text{SnCl})(\text{bpy-}^4\text{bu}_2)]^+$ is very similar to that seen for $[\text{PtClMe}_2(\text{Me}_2\text{SnCl})(\text{bpy-}^4\text{bu}_2)]$, indicating little change in the chemical environment upon removal of the chloro ligand. The ¹H NMR spectrum of the BF_4^- salt is nearly identical with that of the PF_6^- salt, and there is no apparent association of the anions with the cation. The

value of the coupling constant $^2J(^{119}\text{SnH})$ increased from 53.5 Hz for $[\text{PtClMe}_2(\text{Me}_2\text{SnCl})(\text{bpy-}^4\text{bu}_2)]$ to 58.3 Hz for $[\text{PtMe}_2(\text{Me}_2\text{SnCl})(\text{bpy-}^4\text{bu}_2)]^+$, indicating an increase in the *s* character of the tin orbitals used in the Sn-Me bonds for the latter.²⁶ Similarly, there is an increase in the magnitude of $^2J(\text{SnH})_{\text{av}}$ upon extraction of halide from $[\text{PtXMe}_2(\text{Me}_3\text{Sn})(\text{bpy-}^4\text{bu}_2)]$ to give $[\text{PtMe}_2(\text{Me}_3\text{Sn})(\text{bpy-}^4\text{bu}_2)]^+$.

VT ¹H-NMR studies have provided information regarding dynamic solution processes involving the platinum(IV) cationic species. The spectrum of a 1:1 mixture of $[\text{PtClMe}_2(\text{Me}_2\text{SnCl})(\text{bpy-}^4\text{bu}_2)]$ and $[\text{PtMe}_2(\text{Me}_2\text{SnCl})(\text{bpy-}^4\text{bu}_2)]^+$ in CD_3CN shows that exchange of the chloro ligand can occur easily between platinum centers but not between platinum and tin (Scheme 1; note that the cation is probably solvated but the solvent must dissociate rapidly to allow the halide-bridged intermediate to form). However, solutions resulting from the reactions of $[\text{PtXMe}_2(\text{Me}_3\text{Sn})(\text{bpy-}^4\text{bu}_2)] \cdot \text{Me}_3\text{SnX}$ ($\text{X} = \text{Cl, I}$) with 1 equiv of silver(I) also give broadened ¹H NMR spectra at room temperature and in this case exchange occurs between the Me_3Sn groups in $[\text{PtMe}_2(\text{Me}_3\text{Sn})(\text{bpy-}^4\text{bu}_2)]^+$ and Me_3SnX ($\text{X} = \text{Cl, I}$). The broadening is interpreted as due to the reversible exchange of halide between Me_3SnX and the platinum(IV) cation to give $[\text{PtXMe}_2(\text{Me}_3\text{Sn})(\text{bpy-}^4\text{bu}_2)]$, which is known to undergo reversible reductive elimination of Me_3SnX .⁴ The overall exchange process can be represented by Scheme 2 (the cation may well be solvated). The cation $[\text{PtMe}_2(\text{Me}_3\text{Sn})(\text{bpy-}^4\text{bu}_2)]^+$ does not undergo rapid reductive elimination of Me_3Sn^+ , presumably because Me_3Sn^+ is considerably less stable than Me_3SnX (otherwise, it can be considered that a good nucleophile for tin is needed to displace Me_3Sn^+ from platinum).

(23) Onaka, S. *Chem. Lett.* **1978**, 1163.(24) Beagley, B.; McAloon, K.; Freeman, J. M. *Acta Crystallogr.* **1974**, B30, 444.(25) Greene, P. T.; Bryan, R. F. *J. Chem. Soc. (A)* **1971**, 2459.(26) Van den Berghe, E. V.; Van der Kelen, G. P. *J. Organomet. Chem.* **1973**, 59, 175.

Experimental Section

General Considerations. NMR spectra were obtained using a Varian Gemini 300 spectrometer. Spectra were referenced to Me₄Si using the residual proton signals in the deuterated solvent. Assignments of aromatic protons were made using the labeling scheme given in eq 3; only one assignment is given to equivalent nuclei. Molar conductivity measurements were carried out using on a Varian CM-2 molar conductivity apparatus with a cell constant of 10 cm². The instrument was calibrated using a 1.63 × 10⁻³ M solution of Et₃NBr in CH₃CN ($\Lambda = 168.7 \text{ S cm}^2 \text{ mol}^{-1}$).²⁷ All procedures were carried out under an inert atmosphere using dry solvents. An acetonitrile-slush bath was used to cool the reaction mixtures to -40 °C. Acetonitrile was dried by reflux over CaH₂. Precursor platinum(II) and platinum(IV) complexes were prepared as described elsewhere.⁹ Silver salts were purchased from Aldrich and used without further purification.

X-ray Structure Determination of [PtMe₂(Me₂SnCl)(bpy- bu_2)]BF₄. Light yellow rodlike crystals were grown by diffusing pentane into a CH₂Cl₂ solution of the salt at -30 °C. The crystals turned opaque on exposure to air, and hence, they were coated with paraffin oil. A long rod was cut into a suitable size (0.36 × 0.18 × 0.12 mm), wedged inside a Lindemann capillary tube, and flame-sealed for use in diffraction experiments. The density of the crystal was measured by the neutral buoyancy method. The diffraction experiments were carried out on a Siemens P4 diffractometer with XSCANS software package²⁸ using graphite-monochromated Mo K α radiation at 25 °C. The cell constants were obtained by centering 25 high-angle reflections ($23.2 \leq 2\theta \leq 24.9^\circ$). The Laue symmetry 2/m was determined by merging symmetry-equivalent reflections. In total, 3268 reflections were collected in the θ range 1.9–25.0° ($-1 \leq h \leq 13$, $-1 \leq k \leq 13$, $-13 \leq l \leq 13$) in the θ - 2θ scan mode at variable scan speeds (2–10° min⁻¹). Background measurements were made at the ends of the scan range. Three standard reflections were monitored at the end of every 197-reflection collection. The data processing, solution, and initial refinements were done using SHELX-TL-PC programs.²⁹ The final refinements were performed using SHELXL-93 software programs.³⁰ The data were corrected for absorption ($\mu = 6.1 \text{ mm}^{-1}$) using an empirical method involving ψ scans of 15 reflections ($7.0 < 2\theta < 28.3^\circ$). The maximum and minimum transmission factors were 0.183 and 0.104, respectively. For $Z = 2$ in the monoclinic system, the systematic absences ($0k0 = 2n + 1$) indicated that the space group was either $P2_1$ or $P2_1/m$. The mean absolute $e^2 - 1$ value (found 0.671; expected 0.968 and 0.736 for centrosymmetric and noncentrosymmetric) indicates the polar space group $P2_1$. The correctness of choice of the space group was confirmed by the successful refinement of the structure. Anisotropic thermal parameters were assigned and refined for Pt, Sn, Cl and all the methyl carbon atoms attached to Sn and Pt. The two *tert*-butyl groups were found to be disordered. Two different orientations of the methyl carbon atoms were found for each group. The occupancy factors are 0.7/0.3 and 0.5/0.5 for the groups attached to C(15) and C(19), respectively. These two *tert*-butyl groups were treated as idealized tetrahedrons, and a common C–C distance was refined (using DFIX) in the least-squares cycles. Individual isotropic thermal parameters were refined for these carbon atoms. All the hydrogen atoms (except for the *tert*-butyl groups) were placed in the calculated positions, and they were included for the purpose of structure factor calculations only. A common thermal parameter was assigned for the hydrogen atoms and refined in the least-squares cycles. Two different orientations of the fluorine

atoms around the boron atom (occupancies 0.6/0.4) were found in the BF₄⁻ anion. Ideal tetrahedral geometry constraints were imposed for these two orientations using the option SADI. Common isotropic thermal parameters were refined for each model. In the final least-squares refinement cycles on F^2 , the model converged at $R = 0.0459$, $R_w = 0.1074$, and a goodness of fit (S) of 1.049 for 2804 observations with $F_o \geq 4\sigma(F_o)$ and 203 parameters, and $R = 0.0592$, $R_w = 0.1155$ for all 3262 data. In the final difference Fourier synthesis the electron density fluctuates in the range +1.71 to -0.67 e Å⁻³; the top four peaks are associated with the Pt atoms at distances of 0.95–1.18 Å. The least-squares refinements with the Gaussian absorption-corrected data increased the agreement factors and the residual electron density around the Pt atom due to problems of indexing the two cut faces with the crystal inside the capillary tube. The mean and the maximum shift/esd values in the final cycles are 0.006 and 0.058. The Flack parameter was refined to -0.01(2).

[PtMe₂(Me₂SnCl)(bpy- bu_2)]PF₆. [PtClMe₂(Me₂SnCl)(bpy- bu_2)] (300.0 mg, 0.4206 mmol) was dissolved in 6 mL of dry CH₃CN in a dry 50 mL Schlenk tube under a nitrogen atmosphere. The solution was cooled to -40 °C and AgPF₆ (346.0 mg, 0.4206 mmol) was added. A white precipitate formed immediately and the solution changed from light yellow to colorless. The reaction mixture was stirred for 5 min and then filtered through a cold, dry Celite filter into a cold (-40 °C) Schlenk tube. The reaction flask and filter were washed with 3 mL of CH₃CN. The vessel containing the filtrate was removed from the cold bath, and the solvent was removed from the cold flask *in vacuo*. A sticky off-white solid was obtained. The flask was then cooled to -40 °C, and 3 mL of dry toluene was added. The contents of the flask were agitated with a microspatula under a stream of nitrogen. The toluene was then removed *in vacuo*, leaving an off-white powder. The solid was dried *in vacuo* for 6 h: crude yield 318.5 mg, 92.1%. The solid was recrystallized from CH₂Cl₂/pentane under a nitrogen atmosphere: yield 78%. Anal. Calcd for C₂₂H₃₆ClF₆N₂PtSn: C, 32.12; H, 4.41; N, 3.40. Found: C, 32.14; H, 4.28; N, 3.30. ¹H NMR in CD₃CN: δ 0.38 [s, 6H, ²J(¹¹⁹SnH) = 58.3 Hz, ²J(¹¹⁷SnH) = 55.7 Hz, ³J(PtH) = 6.1 Hz, Sn–Me], 1.18 [s, 6H, ²J(PtH) = 53.6 Hz, ³J(SnH)_{av} = 4.64 Hz, Pt–Me], 1.48 [s, 18h, bu_2], 7.80 [dd, 2H, ³J(H^aH^b) = 5.92 Hz, ⁴J(H^bH^d) = 1.98 Hz, H^b], 8.47 [d, 2H, H^d], 8.77 [d, 2H, ³J(PtH) = 15.9 Hz, H^a]. ³¹P NMR in CD₃CN: δ -143.0 [septet, ¹J(PF) = 707.6 Hz, PF₆⁻]. Molar conductivity (7.78 × 10⁻⁴ M solution in anhydrous CH₃CN): $\Lambda = 154 \text{ S cm}^2 \text{ mol}^{-1}$. The same procedure was carried out using 2 equiv of AgPF₆, and the ¹H NMR spectrum of the product was identical with that of [PtMe₂(Me₂SnCl)(bpy- bu_2)]PF₆.

[PtMe₂(Me₂SnCl)(bpy- bu_2)]BF₄. This product was prepared by following the same procedure described for [PtMe₂(Me₂SnCl)(bpy- bu_2)]PF₆, except that a 1:1 mole ratio of [PtMe₂(bpy- bu_2)] to Me₂SnCl₂ was used in place of [PtClMe₂(Me₂SnCl)(bpy- bu_2)] and AgBF₄ was used instead of AgPF₆: yield of off-white powder 87.9%. Crystals suitable for X-ray crystallographic studies were grown by diffusion of pentane into a CD₂Cl₂ solution of the complex at -30 °C over a 3-week period. ¹H NMR in CD₃CN: δ 0.38 [s, 6H, ²J(SnH)_{av} = 57.3 Hz, Sn–Me], 1.17 [s, 6H, ²J(PtH) = 53.6 Hz, Pt–Me], 1.49 [s, 18h, bu_2], 7.81 [dd, 2H, ³J(H^aH^b) = 5.95 Hz, ⁴J(H^bH^d) = 1.89 Hz, H^b], 8.48 [d, 2H, H^d], δ 8.77 [d, 2H, ³J(PtH) = 15.5 Hz, H^a].

NMR Scale Reaction between [PtClMe₂(Me₂SnCl)(bpy- bu_2)] and 0.5 Equiv of AgPF₆. [PtClMe₂(Me₂SnCl)(bpy- bu_2)] (50.0 mg, 0.0701 mmol) was dissolved in CD₃CN (1 mL), and AgPF₆ (8.9 mg, 0.035 mmol) was added. An immediate reaction occurred, and a white precipitate was formed. The solution was then filtered into an NMR tube. ¹H NMR in CD₃CN: δ 0.33 [s(br), 6H, Sn–Me], 1.07 [s, 6H, ²J(PtH) = 55.0 Hz, Pt–Me], 1.46 [s, 18h, bu_2], 7.75 [dd, 2H, ³J(H^aH^b) = 5.92 Hz, ⁴J(H^bH^d) = 1.98 Hz, H^b], 8.44 [d, 2H, H^d], 8.69 [d, 2H, ³J(PtH) = 16.0 Hz, H^a].

(27) Coetzee, J. F.; Cunningham, G. P. *J. Am. Chem. Soc.* **1965**, *87*, 2534.

(28) XSCANS; Siemens Analytical X-Ray Instruments Inc., Madison, WI, 1990.

(29) Le Page, Y. *J. Appl. Crystallogr.* **1987**, *20*, 264.

(30) Sheldrick, G. M. SHELXL-93. *J. Appl. Crystallogr.*, in press.

Reaction of [PtMe₂(Me₂SnCl)(bpy- η -bu₂)]PF₆ with Me₂SnCl₂ in CD₃CN. [PtMe₂(Me₂SnCl)(bpy- η -bu₂)]PF₆ and Me₂SnCl₂ in CD₃CN were dissolved in CD₃CN. ¹H NMR spectra were collected at -40, -20, 0, 20, and 40 °C, the spectra being essentially identical at the four lower temperatures with small changes in signal positions and coupling constants. ¹H NMR in CD₃CN at -40 °C: δ 0.33 [s, 6H, ²J(¹¹⁹SnH) = 58.9 Hz, ²J(¹¹⁷SnH) = 56.2 Hz, ³J(PtH) = 5.5 Hz, Sn-Me], 1.12 [s, 6H, ²J(PtH) = 53.6 Hz, Pt-Me], 1.18 [s, 18H, ²J(¹¹⁹SnH) = 86.6 Hz, ²J(¹¹⁷SnH) = 83.1 Hz, Me₂SnCl₂], 1.43 [s, 18H, η -bu], 7.78 [dd, 2H, ³J(H^aH^b) = 5.82 Hz, ⁴J(H^bH^d) = 1.70 Hz, H^b], 8.50 [d, 2H, H^d], 8.75 [d, 2H, ³J(PtH) = 15.4 Hz, H^a]. ¹H NMR in CD₃CN at 0 °C: δ 0.36 [s, 6H, ²J(¹¹⁹SnH) = 58.3 Hz, ²J(¹¹⁷SnH) = 55.8 Hz, ³J(PtH) = 6.0 Hz, Sn-Me], 1.15 [s, 6H, ²J(PtH) = 53.6 Hz, Pt-Me], 1.19 [s, 18H, ²J(¹¹⁹SnH) = 84.3 Hz, ²J(¹¹⁷SnH) = 80.7 Hz, Me₂SnCl₂], 1.45 [s, 18H, η -bu], 7.77 [dd, 2H, ³J(H^aH^b) = 5.80 Hz, ⁴J(H^bH^d) = 1.71 Hz, H^b], 8.51 [d, 2H, H^d], 8.73 [d, 2H, ³J(PtH) = 15.5 Hz, H^a]. ¹H NMR in CD₃CN at 40 °C: δ 0.40 [s(br), 6H, Sn-Me], 1.19 [s, 6H, ²J(PtH) = 53.3 Hz, Pt-Me], 1.20 [s, 18H, ²J(¹¹⁹SnH) = 81.8 Hz, ²J(¹¹⁷SnH) = 78.5 Hz, Me₂SnCl₂], 1.48 [s, 18H, η -bu], 7.82 [dd, 2H, ³J(H^aH^b) = 5.98 Hz, ⁴J(H^bH^d) = 1.86 Hz, H^b], 8.47 [d, 2H, H^d], 8.77 [d, 2H, ³J(PtH) = 15.5 Hz, H^a].

NMR Scale Reactions between [PtBrMe₂(Me₂SnBr)(bpy- η -bu₂)]₂·Me₂SnBr₂ and AgBF₄. [PtBrMe₂(Me₂SnBr)(bpy- η -bu₂)]₂·0.5Me₂SnBr₂ (30.0 mg, 0.0162 mmol) and AgBF₄ (18.3 mg, 0.0942 mmol) were dissolved in CD₃CN (1 mL) under a nitrogen atmosphere. A white precipitate was formed immediately upon shaking. The solid was removed by filtration through a glass microfiber filter, and the resulting colorless solution was placed in an NMR tube. ¹H NMR in CD₃CN: δ 0.48 [s, 6H, ²J(¹¹⁹SnH) = 64.7 Hz, ²J(¹¹⁷SnH) = 61.9 Hz, ³J(PtH) = 5.8 Hz, PtSn-Me], 1.25 [s, 6H, ²J(PtH) = 54.2 Hz, Pt-Me], 1.38 [s, ²J(¹¹⁹SnH) = 94.0 Hz, ²J(¹¹⁷SnH) = 89.7 Hz, free Me-Sn], 1.47 [s, 18H, η -bu], 7.87 [dd, 2H, ³J(H^aH^b) = 5.89 Hz, ⁴J(H^bH^d) = 1.92 Hz, H^b], 8.52 [d, 2H, H^d], 8.79 [d, 2H, ³J(PtH) = 15.3 Hz, H^a]. The same reaction was carried out using 1 equiv of AgPF₆ and gave a ¹H NMR spectrum which was essentially identical with that described above.

Reaction of [PtClMe₂(Me₃Sn)(bpy- η -bu₂)]·Me₃SnCl with AgBF₄. [PtClMe₂(Me₃Sn)(bpy- η -bu₂)]·Me₃SnCl (100.0 mg, 0.1443 mmol) was suspended in CH₃CN (10 mL) in a dry Schlenk tube. The suspension was cooled to -40 °C, and AgBF₄ (28.1 mg, 0.144 mmol) was added. The solution changed from bright to pale yellow, and a white precipitate formed. The cold solution was filtered through a cold glass microfiber/Celite filter into a second Schlenk tube, which had been cooled to -40 °C. The solvent was removed from the cold solution *in vacuo*: yield 92 mg. A sample of the solid gave a cloudy solution in CD₃CN, which was filtered through a glass microfiber filter to give a yellow solution. ¹H NMR in CD₃CN at 20 °C: δ -0.14 [s(br), 9H, MeSn-Pt], 0.58 [s(br), 9H, Me₃SnCl], 1.09 [s, 6H, ²J(PtH) = 56.9 Hz, Pt-Me], 1.46 [s, 18H, η -bu], 7.79 [dd, 2H, ³J(H^aH^b) = 5.89 Hz, ⁴J(H^bH^d) = 1.98 Hz, H^b], 8.44 [d, 2H, H^d], 8.78 [d, 2H, ³J(PtH) = 15.94 Hz, H^a]. ¹H NMR in CD₃CN at -40 °C: δ -0.25 [s, 9H, ²J(¹¹⁹SnH) = 53.6 Hz, ²J(¹¹⁷SnH) = 51.2 Hz, ³J(PtH) = 13.46 Hz, MeSn-Pt], 0.56 [s, 9H, ²J(¹¹⁹SnH) = 66.0 Hz, ²J(¹¹⁷SnH) = 64.5 Hz, Me₃SnCl], 1.09 [s, 6H, ²J(PtH) = 56.6 Hz, ³J(SnH) = 4.7 Hz, Pt-Me], 1.47 [s, 18H, η -bu], 7.74 [dd, 2H, ³J(H^aH^b) = 5.93 Hz, ⁴J(H^bH^d) = 1.93 Hz, H^b], 8.45 [d, 2H, H^d], 8.75 [d, 2H, ³J(PtH) = 15.8 Hz, H^a].

Reaction of [PtIme₂(Me₃Sn)(bpy- η -bu₂)]·Me₃SnI with AgPF₆. The same procedure was followed as described for the reaction of [PtClMe₂(Me₃Sn)(bpy- η -bu₂)]·Me₃SnCl with AgBF₄, except [PtIme₂(Me₃Sn)(bpy- η -bu₂)]·Me₃SnI (100 mg, 0.0931 mmol) and AgPF₆ (23.6 mg, 0.0931 mmol) were used: yield

88 mg. ¹H NMR in CD₃CN at 20 °C: δ -0.14 [s(br), 9H, MeSn-Pt], 0.61 [s(br), 9H, Me₃SnI], 1.10 [s, 6H, ²J(PtH) = 56.9 Hz, Pt-Me], 1.46 [s, 18H, η -bu], 7.78 [dd, 2H, ³J(H^aH^b) = 5.86 Hz, ⁴J(H^bH^d) = 1.95 Hz, H^b], 8.43 [d, 2H, H^d], 8.77 [d, 2H, ³J(PtH) = 15.93 Hz, H^a]. ¹H NMR in CD₃CN at -40 °C: δ -0.27 [s, 9H, ²J(¹¹⁹SnH) = 53.2 Hz, ²J(¹¹⁷SnH) = 51.0 Hz, ³J(PtH) = 13.3 Hz, MeSn-Pt], 0.49 [s, 9H, ²J(¹¹⁹SnH) = 64.6 Hz, ²J(¹¹⁷SnH) = 67.5 Hz, Me₃SnI], 1.00 [s, 6H, ²J(PtH) = 56.6 Hz, ³J(SnH) = 4.9 Hz, Pt-Me], 1.42 [s, 18H, η -bu], 7.72 [dd, 2H, ³J(H^aH^b) = 5.89 Hz, ⁴J(H^bH^d) = 1.92 Hz, H^b], 8.42 [d, 2H, H^d], 8.71 [d, 2H, ³J(PtH) = 15.6 Hz, H^a].

Reaction of [PtIme₂(Me₃Sn)(bpy- η -bu₂)] with AgBF₄. The same procedure was followed as described for the reaction of [PtClMe₂(Me₃Sn)(bpy- η -bu₂)]·Me₃SnCl with AgBF₄ except [PtIme₂(Me₃Sn)(bpy- η -bu₂)] (100 mg, 0.128 mmol) and AgBF₄ (24.8 mg, 0.128 mmol) were used: yield 77 mg. ¹H NMR in CD₃CN at -40 °C: δ -0.29 [s, 9H, ²J(¹¹⁹SnH) = 53.1 Hz, ²J(¹¹⁷SnH) = 50.8 Hz, ³J(PtH) = 13.2 Hz, MeSn-Pt], 1.00 [s, 6H, ²J(PtH) = 56.9 Hz, ³J(SnH) = 4.9 Hz, Pt-Me], 1.40 [s, 18H, η -bu], 7.69 [dd, 2H, ³J(H^aH^b) = 5.86 Hz, ⁴J(H^bH^d) = 1.93 Hz, H^b], 8.42 [d, 2H, H^d], 8.71 [d, 2H, ³J(PtH) = 15.5 Hz, H^a].

Reaction of [PtIme₂(bpy- η -bu₂)] with *in situ* Generated Me₃SnBF₄. To a solution of Me₃SnCl (40.4 mg, 0.203 mmol) in CH₃CN (20 mL) was added AgBF₄ (39.4 mg, 0.203 mmol), and a white precipitate formed immediately. The colorless solution was cooled to -40 °C, and [PtIme₂(bpy- η -bu₂)] (100.0 mg, 0.2026 mmol) was added to give a yellow solution. The cold solution was filtered through a glass microfiber/Celite filter into a second cold Schlenk tube. The solvent was removed from the cold solution *in vacuo*, leaving a yellow-orange solid: yield 122 mg. ¹H NMR in CD₃CN at -40 °C: δ -0.26 [s, 9H, ²J(¹¹⁹SnH) = 53.5 Hz, ²J(¹¹⁷SnH) = 51.2 Hz, ³J(PtH) = 13.4 Hz, MeSn-Pt], 1.02 [s, 6H, ²J(PtH) = 56.3 Hz, ³J(SnH) = 4.7 Hz, Pt-Me], 1.42 [s, 18H, η -bu], 7.74 [dd, 2H, ³J(H^aH^b) = 5.92 Hz, ⁴J(H^bH^d) = 1.92 Hz, H^b], 8.43 [d, 2H, H^d], 8.72 [d, 2H, ³J(PtH) = 15.9 Hz, H^a].

Reaction of [PtIme₂(Me₃Si)(bpy- η -bu₂)] with Silver Salts. [PtIme₂(Me₃Si)(bpy- η -bu₂)] (100.0 mg, 0.1442 mmol) was dissolved in 10 mL of CH₃CN. The yellow solution was cooled to -40 °C, and AgBF₄ (28.1 mg, 0.144 mmol) was added. An immediate reaction occurred to give a white precipitate and a colorless solution. The solution quickly darkened to deep yellow. The solution was filtered cold (-40 °C), and the solvent was removed *in vacuo* from the solution: yield of orange solid 52 mg. ¹H NMR in CD₃CN at -40 and 20 °C showed a complex mixture and no evidence of a Me₃Si-Pt signal. Similar results were obtained for reactions carried out in THF at -78 °C. In an NMR tube reaction, [PtIme₂(Me₃Si)(bpy- η -bu₂)] was reacted with 1 equiv of AgPF₆ in CD₃CN at -40 °C and the ¹H NMR spectrum was acquired without warming the sample. The -40 °C spectrum was complicated and showed no Me₃Si-Pt signal. Several Me-Si signals appeared (0.02, 0.14, 0.16, and 0.19 ppm), indicating a complicated decomposition process.

Acknowledgment. We thank the NSERC (Canada) for financial support.

Supporting Information Available: Tables of thermal parameters, H atom positional parameters, torsion angles, and least-squares planes for [PtMe₂(Me₂SnCl)(bpy- η -bu₂)]BF₄ (6 pages). This material is contained in many libraries on microfiche, immediately follows this article in the microfilm version of the journal, can be ordered from the ACS, and can be downloaded from the Internet; see any current masthead page for ordering information and Internet access instructions.

OM950591F